

1

2

3

4

5

6

A physical demonstration of the increase

7

in global surface energy due to increasing P_{CO_2}

8

9 Hugo F. Franzen, Professor Emeritus. Dept. of Chem., Iowa State University, Ames, IA 50011

10 Stefan Franzen. Dept. of Chem.. North Carolina State University, Raleigh, NC 27695

11

12 Corresponding author: Stefan Franzen (franzen@ncsu.edu)

13

14 **Abstract**

15 Although study of the effect of energy-absorbing gases in our atmosphere has a two-
16 hundred year history and an unequivocal explanation based on scientific observation and theory,
17 a significant fraction of the public and even a few scientists doubt the correlation between the
18 increasing the partial pressure of atmospheric carbon dioxide (P_{CO_2}) and the observed increase in
19 terrestrial temperature over the past 120 years. Although the basic science showing that CO_2 would
20 absorb the infrared radiation emitted by the earth produce a surface-warming effect was first
21 calculated by Arrhenius in 1896, the issue was neglected by the scientific community for decades.
22 Today there are ample climate models of the climactic effects arising from the forcing term of
23 increasing P_{CO_2} . In this paper we follow Arrhenius' concept, although we use the HITRAN
24 database as the input to prove the connection between earth's surface temperature and atmospheric
25 absorption of terrestrial radiation in a direct manner that the reader can also implement. The spectra
26 of CO_2 are enormously complicated, broadened by Fermi Resonance, and intense because of the
27 quantum coupling of the rotation of CO_2 to its bending. Using an on-line database for the
28 transitions of CO_2 the reader will easily be able to show that CO_2 reduces the transmittance of the
29 Earth's thermal radiation through the atmosphere, which in turn results in heating of the surface.
30 The model does not make any predictions other than that the global temperature will increase as a
31 function of P_{CO_2} . The result is at the intersection of Physics, Atmospheric Science, and Psychology
32 since the demonstration is a powerful tool that will give scientists the impetus to reach out to the
33 public with lucid explanations based on physical principles.

34

35 **Introduction**

36 There is a need for a clear statement of the quantitative connection between increasing
37 atmospheric carbon dioxide (CO₂) levels and changes in the global energy balance. While this
38 connection is widely accepted among scientists, the economic implications of the problem have
39 resulted in widespread denial elsewhere in society. Recent events, such as the cataclysmic fires in
40 Australia, Amazonia[1] and California,[2] the hot spot in the Pacific Ocean responsible for killing
41 millions of fish[3] and the accelerated pace of arctic and Antarctic melting[4] highlight the urgency
42 of the problem. These changes are predicted to become the new normal, but the larger danger arises
43 as the earth approaches tipping points, such as the conversion of northern boreal forests from net
44 carbon uptake to sources of carbon emission[5] or the drying out of the Amazon basin.[6] These
45 events put a spotlight on the need for increased understanding of the earth's energy balance. In
46 spite of overwhelming evidence, denial is as active as at any time in the past century by those who
47 fear that change will result in economic dislocation. In fact, the imposition of political
48 considerations on science has increased in recent years.[7] This situation calls for a first-principles
49 approach that gives scientists the tools to address an issue that may be outside their specialized
50 field of study.

51 There is an enormous body of work by climatologists that substantiates the connection
52 between a warming trend and the dramatic rise in CO₂ ppm over the past 120 years. Although
53 skeptics have questioned the significance and magnitude of the trend toward increasing global
54 average temperature, recent record temperatures, and melting of polar ice at an accelerated pace
55 have all but obliterated the argument that temperature rise is not a concern. Moreover, there is no
56 question that the increase in CO₂ partial pressure is a consequence of human activity, principally
57 the combustion of fossil fuels. Therefore, the last bastion of the critics is to question the link

58 between the temperature rise and the increase in P_{CO_2} . That link is considered a result of the
59 *greenhouse gas* effect, which is specifically caused by the strong absorption of the earth's thermal
60 radiation by carbon dioxide in the range 9-17 μ .

61 The physics of *thermal radiation* is taught as the initial motivation for Quantum Mechanics
62 in most Physical Chemistry curricula.[8] Textbooks refer to Blackbody Radiation but the name
63 blackbody can be confusing. We prefer the term *thermal radiation* since it describes how the
64 radiation emitted stars and planets permits each to have a different temperature at equilibrium.
65 Because the subject is introduced with a focus on Planck's justification for quantized radiation,
66 the other aspects of the theory are often omitted in Chemistry curricula, despite their importance.
67 For example, Kirchoff's law of absorption states that perfect absorbers are black in color because
68 all wavelengths are absorbed, hence the name blackbody. In Kirchoff's model, emission depends
69 on wavelength and is a function of temperature only. These laws are statements about ideal spheres
70 used to explain how the planets, stars and other celestial bodies can exist in thermal equilibrium at
71 different temperatures. In the 1860s scientists were trying for the first time to reconcile
72 thermodynamics and radiation physics. The question was: how can two objects be at equilibrium,
73 yet be at different temperatures? The answer was: thermal radiation is a universal phenomenon,
74 and it means that every object in the universe radiates at a wavelength that is inversely proportional
75 to its temperature. Stars provide visual examples of thermal radiation. Stars would be blackbodies
76 if it were not for the fact that atoms are an ionized plasma so there are many thousands of
77 absorption lines. The emission of stars is far from perfect because of the absorption by hydrogen,
78 helium, and a surprising range of other elements that form as the stars age. The circa 25,000 intense
79 narrow bandwidth absorption bands of atomic transitions in our Sun are known as Fraunhofer
80 lines.

81 The empirical relationships that describe the radiation and temperature of stars and planets
82 have been known since the 1880's and are given the names, the Stefan-Boltzmann law[9] and the
83 Wien displacement law.[10] The Stefan-Boltzmann law states that

$$84 \quad F = \sigma T^4 \quad (1)$$

85 Where F is the radiation flux from the surface in W/m^2 , T is absolute temperature and $\sigma = 5.678 \times$
86 $10^{-8} \text{ W}/\text{m}^2/\text{K}$ is known as the Stefan-Boltzmann constant. Using only the above law, the radius
87 of the sun, the radius of the earth's orbit and the temperature of the sun, one can calculate an
88 accurate temperature of the surface of a bare earth (without an atmosphere). To obtain an accurate
89 result we must include albedo, A , which is the reflection of some of the radiation by the earth. If
90 one uses the values $A = 0.3$, $R_{sun} = 7 \times 10^8 \text{ m}$, $R_{orbit} = 1.5 \times 10^{11} \text{ m}$ and $T_{sun} = 5780 \text{ K}$, one
91 obtains $T_{bare\ earth} = 255 \text{ K}$. These parameters are quite reliable. The albedo is the most difficult to
92 measure, hence it is a parameter that could change somewhat depending on the composition of the
93 atmosphere we call attention to it as an assumption of our model.

$$94 \quad T_{bare\ earth} = \sqrt{\frac{\sqrt{(1-A)}R_{sun}T_{sun}}{2R_{orbit}}} \quad (2)$$

95 This formula works well for planets that have little or no atmosphere, such as Mars or Neptune.
96 This application assumes that the planet rotates about an axis with an azimuthal angle close enough
97 to perpendicular to the plane of the orbit that the energy is equally distributed over the surface. It
98 is not appropriate for Mercury, which does not rotate about a planetary axis. It also fails for the
99 surface of Earth, which is more than $30 \text{ }^\circ\text{C}$ warmer because of its absorbing atmosphere. The earth
100 would be a giant snowball if it lacked a CO_2 atmosphere.

101 The emission wavelength of thermal radiation by celestial bodies is inversely proportional
102 to the steady-state temperature. This inverse proportionality was observed empirically using a
103 platinum filament in the 1860s and later called the Wien displacement law,

$$104 \quad \lambda_{max}T = 2.88 \times 10^6 \text{ nm} - K \quad (3)$$

105 From this equation we can calculate that the maximum emission wavelength of the sun and earth
106 are 524 nm and 11,300 nm, respectively.

107 It has been recognized for well over 150 years that the surface temperature of a planet will
108 be strongly affected by the presence of an atmosphere. The delay in recognition of the importance
109 of energy-absorbing gases in Earth's atmosphere by the scientific community is a discouraging
110 fact that exemplifies how self-deception can impede the progress of the search for the truth.[11]
111 The concern raised by Svante Arrhenius in an article published in 1896[12] has stood the test of
112 time.[13] Although Arrhenius had a limited data set, obtained mainly from Langley's observations
113 of infrared radiation from the moon,[14] he was able to use those data and Stefan-Boltzmann law
114 to estimate the increase in temperature at the surface of the earth that would be caused by an
115 increase in CO₂ partial pressure. Today the International Panel on Climate Change (IPCC) and
116 hundreds of research groups publish both measurements and simulations that document the
117 correlation with great accuracy. Of course, instead of a few points of lunar radiation scribbled in a
118 notebook, modern atmospheric science is based on satellite data and quantum theory of transitions.

119 It is interesting from the point of view of the history of science that Svante Arrhenius'
120 result was disputed from the very beginning by Knut Ångström, the son of the famous Jonas
121 Ångström for whom the unit of atomic length was named.[15] In an ostentatious experiment Knut
122 Ångström traveled to the island of Tenerife in 1900 and climbed Pico de Teide to test whether pure

123 CO₂ would absorb more incident solar radiation than air at the same pressure. The study describes
124 how tubes containing pure CO₂ gas and air, both at atmospheric pressure, were compared by
125 detecting the transmittance of the sun's radiation through the tube on the mountain top. However,
126 the great expense to reach high elevation, where the equatorial sun's radiation would be relatively
127 intense, was unnecessary. The heating of the earth's surface by CO₂ absorption does not depend
128 on incident solar radiation. CO₂ absorbs the long-wavelength emission from the earth, and very
129 little of the short wavelength emission from the sun. In that paper, Ångström did briefly describe
130 an experiment by his *colleague* Koch to measure the absorption of infrared thermal radiation
131 emitted at 373 K passing through a CO₂ atmosphere. There is an apparent discrepancy by a factor
132 of 15 in both the cross-sectional number density and the magnitude of the change in absorbance
133 when the CO₂ pressure was reduced in the result attributed to Koch. The publication did not
134 mention that Mr. Koch was an undergraduate student. There was no follow-up or validation of Mr.
135 Koch's claim by experienced researchers. Despite the apparent flaws and second-hand reporting,
136 Ångström's article appears to have ended any debate for decades afterwards. In 1938 there were
137 discoveries in atmospheric monitoring[16] and an increasing understanding of CO₂ absorption of
138 infrared light[17,18] both of which showed a glimmer of interest for the deeper problem posed.
139 However, the consequences of absorption of energy by the atmosphere were ignored until Keeling
140 began measuring the P_{CO_2} in the atmosphere in 1958.[19] By that time, there was a measurable and
141 significant annual increase in CO₂ pressure in the atmosphere. By the 1960s, there was a growing
142 consensus that the increase in P_{CO_2} in the atmosphere was correlated with a temperature increase at
143 the earth's surface. Although the great majority of scientists agree that there is a correlation
144 between P_{CO_2} and the documented temperature increase, there is financial and political support for
145 a small minority of scientists who argue against such a correlation. To be generous in our

146 interpretation Ångström was deceiving himself by means of his poorly conceived experiment. It
147 is evident that self-deception exists in science, and it is particularly prevalent in areas of great
148 current interest. Consequently, there is a need for physical science to provide a basic understanding
149 of the issue that can be spread to the widest possible audience.

150 An enormous amount of work and thought that has gone into climate science including
151 long-term implications based on studies of geology, paleogeology and oceanography.[20] The
152 scientific objections to the link between anthropogenic CO₂ on the increasingly indisputable rising
153 temperature of the earth's surface have been disproven.[21-26] However, the question remains:
154 how can the scientific community disseminate an understanding of the alarming trends in a clear
155 and understandable fashion? Computer simulations have great value for understanding marine and
156 atmospheric cycles involved in the redistribution of energy throughout the geosphere, both in terms
157 of chemical cycles, heat transfer and radiation balance. These methods have been applied to the
158 effects of forcings and feedback loops on the energy balance in the atmosphere The collective
159 efforts of many scientists have contributed to resources such as the Community Atmospheric
160 Model (CAM3.0).[27-30] A second major initiative is the Coupled Model Intercomparison Project
161 (CMIP).[31-34] These are open source computational models that include the oceans, ice, land
162 and their interaction with the atmosphere useful for climate scientists.[35] A complete model of
163 the effects of changes in any gas added to the atmosphere progresses from energy balance methods
164 to complete global descriptions using finite difference methods on a grid.[36] These models
165 include the full range atmospheric phenomena included in the water cycle, all relevant gases and
166 the role of oceans and land, to describe the radiation balance. The great majority of scientists agree
167 with the fundamental conclusion that increasing CO₂ in the atmosphere is a forcing term that is
168 correlated with the temperature increase at the earth's surface.[27-29,37-42]The treatment

169 presented here provides an appreciation of the starting point for such simulations and would permit
170 a scientist with any related background to defend the basic ideas without necessarily understanding
171 the details of a complex computer simulation. It certainly helps that the result of the simple model
172 presented here is in reasonable agreement with the models.

173 Our approach is to employ a simple radiation equilibrium model that explains the
174 greenhouse gas effect. The application includes a static model that properly calculates the surface
175 temperature of the earth at a given fixed pressure of CO₂. The entire calculation is given in the
176 Supporting Information, along with an Excel and python script showing the step-by-step
177 calculation of temperature from an input CO₂ absorption spectrum from HITRAN and P_{CO_2} . In the
178 Supporting Information we also present an analytic differential model that explains how
179 continually emitting CO₂ leads to an imbalance in the radiation flux at the top of the atmosphere,
180 which in turn causes the earth to heat continuously in the presence of constant incident solar
181 radiation. We neglect scattering and reflection within the atmosphere, which greatly simplifies the
182 treatment of radiation fluxes. The sole external variables are albedo and water vapor.

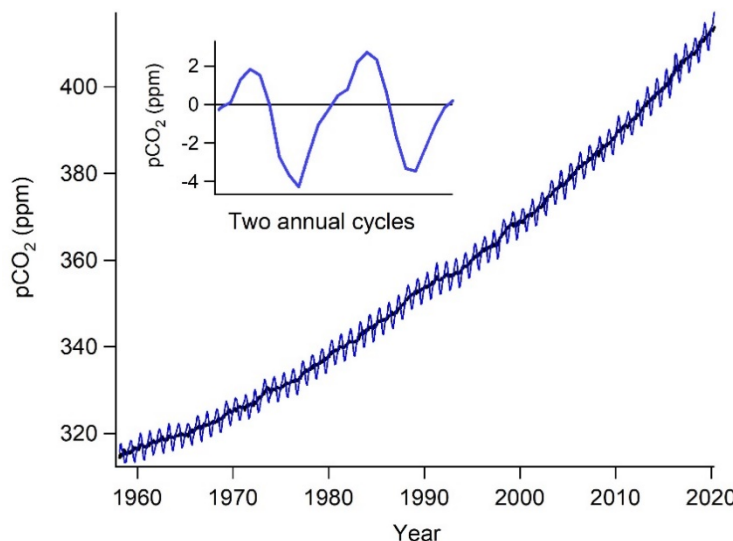
183 A reduction in transmittance due to an increase in energy-absorbing gas concentration will
184 require an increase in the earth's surface temperature to compensate. The small net decrease in
185 emission of ~ 0.85 W/m² in the spectral regions where earth emits radiation are caused by mainly
186 by CO₂ absorption that creates a radiative forcing.[42,43] A great deal of effort has gone into
187 measuring and modeling radiative forcings as a function of CO₂ concentration and distribution in
188 the atmosphere.[44-49] Rather than calculating the CO₂ spectrum from first principles. To
189 demonstrate this in a simple model we will use a publicly available database to obtain absorption
190 transitions and their intensities. Computer codes such as MODTRAN also use the *high-resolution*
191 *transmission* molecular absorption database (HITRAN) database to calculate radiation transfer in

192 the atmosphere using either line-by-line or band models, respectively.[50] Comprehensive
193 simulations are usually implemented in a layer-by-layer approach to account for all terms,
194 absorption, emission and scattering in each layer. Non-specialists can learn to access the database
195 and determine the spectrum of CO₂ from the tabulated values for a much simpler calculation that
196 we have implemented in an Excel spreadsheet, an IgorPro spreadsheet, or using python scripts
197 where we use only the output absorption intensities that are available in HITRAN. These are freely
198 available in the Supporting Information.

199 *Experimental evidence for increase in the concentration of atmospheric CO₂*

200 The Keeling Curve shown in Figure 1 consists of observations of the measured ppm of
201 CO₂ in the atmosphere at Moana Loa, Hawaii versus time in years.[51] The data for CO₂ ppm since
202 1958 have been

203 in ongoing web
204 maintained by
205 Institute. There are
206 discernable
207 variations of the
208 level. There is a
209 annual variation



summarized
publications
Scripps
two easily
temporal
CO₂ ppm
periodic
(shown in

218 the inset) superimposed on a super-linear increase. The fluctuations about the global average are
219 due to local sources and sinks of CO₂ resulting from seasonal variation in plant growth and decay,
220 industry, heating of buildings in the winter other aspects of the carbon cycle. These are continually
221 measured by the GLOBALVIEW network of total carbon measurement spectroscopy centers.[52]
222 The available data, taken over a large number of altitudes at different latitudes by NOAA, lead us
223 to conclude that mixing is rapid in the atmosphere, which means that the Keeling curve is an
224 accurate representation of global trends in atmospheric CO₂ concentration. [19]

225
226

227 Figure 1. The Keeling Curve. The Moana Loa data are compared with data collected at latitudes between
228 the Antarctic and the arctic and at high altitudes. These data demonstrate that the long term global
229 increase in CO₂ ppm is accurately measured at Moana Loa.[19]

230 The underlying long-term increase shown in black in Figure 1 is super-linear, but not
231 exponential. When fit to a quadratic polynomial in units of months, m :

$$232 \quad \delta P_{CO_2}(m) = 2.601 (\pm 0.244) + 0.06372 (\pm 0.00152)m + 9.029 \times 10^{-5} - 5 (\pm 1.98 \times 10^{-6}) m^2$$

233 From the linear term, we can estimate:

$$234 \quad \frac{\delta P_{CO_2}(m)}{\delta m} = 0.0637 \quad (4)$$

235 The periodic component is quite smooth, which implies that the mixing time of carbon
236 dioxide in the atmosphere is short relative to the time of seasonal change. The Keeling Curve data
237 collected in the last decade are essentially linear with a slope of 2.1 ppm per year. This corresponds
238 to a global atmospheric increase of about 16 billion tons per year whereas economic data
239 demonstrate that the worldwide annual combustion of fossil fuels produces more than twice that
240 amount. It is apparent that approximately 50% of the CO₂ produced from combustion sources is
241 taken up by the world's oceans. Far from helping to solve any problems caused by the atmospheric
242 effects, the ocean uptake of CO₂ contributes to acidification, which may have future adverse
243 consequences for phytoplankton and global O₂ levels if current trends continue.

244 ***Experimental evidence for absorption by atmospheric CO₂***

245 Between 1970 and 1980 the NASA Nimbus IV satellite circled the earth at about 1100 km
246 above the surface to collect atmospheric data. The principal absorbing and emitting species in the
247 spectrum at the top of the atmosphere are water vapor (spread over most of the spectrum), carbon
248 dioxide (between 590 and 790 cm⁻¹), ozone (between 1000 and 1100 cm⁻¹), and methane (between
249 1250 and 1450 cm⁻¹). A calculated spectrum for the earth's atmosphere matches the experiment
250 extremely well.[53] Zhong and Haigh calculated the outgoing radiation at the top of the

251 atmosphere including both infrared absorption and emission, using a layer-by-layer approach.
252 Although it is great simplification, we show that a simple absorption model can also describe the
253 forcing by CO_2 that results from the reduction in transmittance as P_{CO_2} increases. Across the range
254 from $0 - 2,400 \text{ cm}^{-1}$ the absorption spectrum consists primarily of absorption by CO_2 and H_2O
255 vapor.[53] We show further that it is a good approximation to treat different absorbing species as
256 additive constituents in a gas mixture. This approach is similar to that employed by Arrhenius, but
257 with much better data thanks to HITRAN and the hindsight of more than 120 years that justifies
258 the Planck theory and the integral of the Planck distribution known as the Stefan-Boltzmann law
259 (Eqn. 1). Given the complexity of many models, a convincing physical demonstration must be
260 feasible for even a non-specialist to implement a calculation to prove the validity of the correlation.
261 We use a spreadsheet implementation of the calculation of the surface temperature of the earth,
262 which is complemented by visualization and computation tools.

263 In solution chemistry absorption is calculated using the Beer-Lambert Law in the form
264 $\ln(I/I_0) = -kc\ell$, where variables are the intensity, I , the molar absorptivity, k , the path length, ℓ ,
265 and concentration, c . In fact, since $I/I_0 = \rho/\rho_0$, radiation fluxes are affected by the same law.
266 Both ratios are equal to the transmittance, τ . The concentration, c , is not constant in an atmospheric
267 column. Calculation of intensity involves an integral over the variable c as a function altitude. The
268 value of this integral is the number of moles of absorber in the column length, called the cross-
269 sectional number density, u , given here in units of moles of absorbing gas per m^2 . The quantity u
270 for the earth's atmosphere is related to the atmospheric pressure, P , and the molecular weight of
271 absorbing gas, M_{m,CO_2} , by $u = P_{CO_2}/gM_{m,CO_2}$ where g is the acceleration of gravity. The mass of
272 CO_2 in the atmosphere is

273
$$m_{CO_2} = \frac{P_{atm}A}{g}x_{CO_2} \quad (5)$$

274 where, $A = 1 \text{ m}^2$, $g = 9.8 \text{ m/s}^{-2}$, $P_{atm} = 1.013 \times 10^5 \text{ N/m}^2$, and $x_{CO_2} = 4.2 \times 10^{-4}$. This mass is
275 converted to moles using the molar mass of CO_2 ($M_{m,CO_2} = 0.044 \text{ kg/mol}$). Using these quantities,
276 we can calculate the limiting cross-sectional number density for CO_2 per m^2 for absorption up to
277 the top of the atmosphere as

278
$$u_{TOA,CO_2} = \frac{m_{CO_2}}{M_{m,CO_2}A} \quad (6a)$$

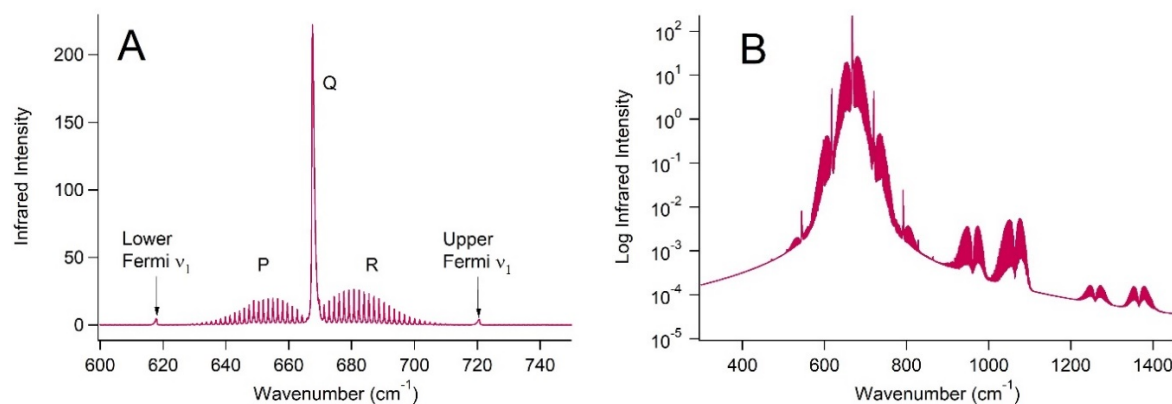
280 The cross-section number density is $u_{TOA,CO_2} = 98.7$ moles per square meter. We can also use
281 Eqn. 5 to write this cross-sectional density as a proportionality to x_{CO_2} .

282
$$u_{TOA,CO_2} = \frac{P_{atm}}{M_{m,CO_2}g}x_{CO_2} \quad (6b)$$

283 ***Computation of CO_2 spectra***

284 To calculate the rate of global energy change due to increasing CO_2 pressure we need to
285 integrate the transmittance of all CO_2 transitions that absorb a fraction of the earth's emission.
286 Infrared absorption by molecules in the gas phase results from simultaneous vibrational and
287 rotational transitions, so-called rovibrational transitions. Figure 2 shows that CO_2 has three
288 infrared-active vibrational modes, the asymmetric stretch, ν_3 at $2,349 \text{ cm}^{-1}$ and two orthogonal
289 bending modes, ν_2 , each at 667 cm^{-1} . [54] The asymmetric stretch is far removed from the peak
290 of the Planck emission of the earth at 288 K, which is approximately at 11,000 nm or 900 cm^{-1} .
291 Since it absorbs in region very weak region of the earth's thermal flux the absorption has little

292 effect on temperature. The symmetric stretch, ν_1 , is not observed in the infrared spectrum, but is
293 Raman active. Both ν_1 and $2\nu_2$ have an expected transition energy of 1334 cm^{-1} . This coincidence
294 of two modes that have the same symmetry leads to a phenomenon known as Fermi resonance,
295 which splits the band energy to give two observed Raman bands at 1285 cm^{-1} and 1388 cm^{-1} . As
296 a consequence, there are two additional bands in the ν_2 infrared spectrum with origins at 667 ± 50
297 cm^{-1} or $\sim 620\text{ cm}^{-1}$ and $\sim 720\text{ cm}^{-1}$ as shown in Figure 2A. Because the CO_2 bending mode involves
298 angular momentum from the bending vibration, all three branches of rotational-vibrational
299 spectrum, P, Q, and R are infrared active.



300
301 Figure 2. A. Infrared absorption spectrum of the bending mode of CO_2 obtained from data in the
302 HITRAN database, including the Fermi splitting, which is indicated as the upper and lower Fermi levels.
303 [55] B. The CO_2 absorption spectrum from $300\text{-}1450\text{ cm}^{-1}$ shown on a logarithmic scale. The lines
304 obtained from the HITRAN database were dressed with Gaussian lineshapes that included a collisional
305 broadening of 0.13 cm^{-1} . [56]

306 The two bending modes of CO_2 have additional infrared absorptions owing to Fermi
307 resonance, which are also indicated in Figure 2. A Fermi resonance is a quantum mechanical result
308 of the interaction of a two-quantum transition in the bending mode with the symmetric stretching
309 mode. The two-quantum transition is totally symmetric because the square of any spectroscopic

310 term is totally symmetric. The interaction gives rise to a splitting resulting from the sum and
311 difference interaction energy between these two transitions. The splitting was first observed in the
312 Raman spectrum of the symmetric stretching band of CO₂ in 1930 by Enrico Fermi.⁵⁷ Because the
313 coupling is a mutual effect, the splitting is observed in the infrared transition of the bending mode
314 as well. The Fermi resonance splitting energy is ~100 cm⁻¹ so that the consequence of Fermi
315 resonance in the infrared spectrum is a new set of absorptions with the entire set of rovibrational
316 transitions located at 618 cm⁻¹ and 720 cm⁻¹ on either side of the main Q-band at 667 cm⁻¹ (see
317 Figure 2A).

318 It is convenient to obtain spectral intensities for CO₂ from the HITRAN database. There
319 are approximately 67,700 transitions between 150 and 2400 cm⁻¹ for natural abundance CO₂. Many
320 of the absorption bands are very weak. Precisely because they are weak, these absorption bands
321 are far from saturated. The CO₂-only model calculation quantitatively confirms that many weak
322 lines give rise to increasing absorption throughout the entire range of CO₂ partial pressure. Given
323 the Gaussian line width of $\gamma = 0.13$ cm⁻¹ the spacing of these transitions is so dense that there is a
324 continuous region of absorption extending from 400 – 1000 cm⁻¹, which includes the peak region
325 for the earth's thermal radiation. Only the central region is saturated. The wings of the rotational
326 branches and Fermi resonance associated rotational lines are far from saturated at the current
327 concentration of 410 ppm obtained from the Keeling curve in Figure 1.[51] These features are
328 evident in Figure 2A, which shows the progression of rovibrational bands in both the high and low
329 energy directions and the Fermi-resonance origins. In the following we calculate the transmittance
330 of these bands under atmospheric conditions as a function of CO₂ ppm. The skeptic's *saturation*
331 *hypothesis*, which states that increasing CO₂ will not affect the absorption of energy from the earth
332 has been addressed by Schildknecht in a recent article describing a spectroscopic and radiation

333 model for the energy-absorbing gas effect.[57] We build on this work by providing a quantitative
334 calculation of the transmittance of the atmosphere under terrestrial conditions. The intense central
335 Q-band is saturated but large spectral flanking regions of the P- and R-band are not near saturation.
336 The overall effect is nearly a linear dependence on CO_2 ppm up to $P_{CO_2} \sim 0.0006$. There is some
337 curvature by $P_{CO_2} \sim 0.001$ atm, i.e. 1,000 ppm, but the saturation region begins at several thousand
338 ppm of CO_2 .

339 **Methods**

340 Assuming emission of a point source on the surface of the earth into a vertical column of
341 the atmosphere with an area of 1 meter squared, the magnitude of the flux, $F_o(T)$, can be compared
342 to the flux of thermal radiation in the presence of the angle dependence of CO_2 absorption,

$$343 \quad F_{TOA}(T) = 2\pi hc^2 \int_0^1 \int_0^\infty \frac{\tilde{\nu}^3 e^{-k_{CO_2}(\tilde{\nu})u_{CO_2}/\mu}}{e^{hc\tilde{\nu}/kT} - 1} d\tilde{\nu} \mu d\mu \quad (7)$$

344 where $\mu = \cos \theta$. Combining the above results, the calculated flux transmittance at τ_{atm} is

$$345 \quad \tau_{atm} = \frac{F_{TOA}(T)}{F_o(T)} \quad (8)$$

346 To calculate F_o one assumes that $e^{-k_{CO_2}(\tilde{\nu})u_{CO_2}} = 1$. The transmittance is a function of the CO_2 ppm
347 because u_{CO_2} depends on the concentration of CO_2 in Eqn. 7.

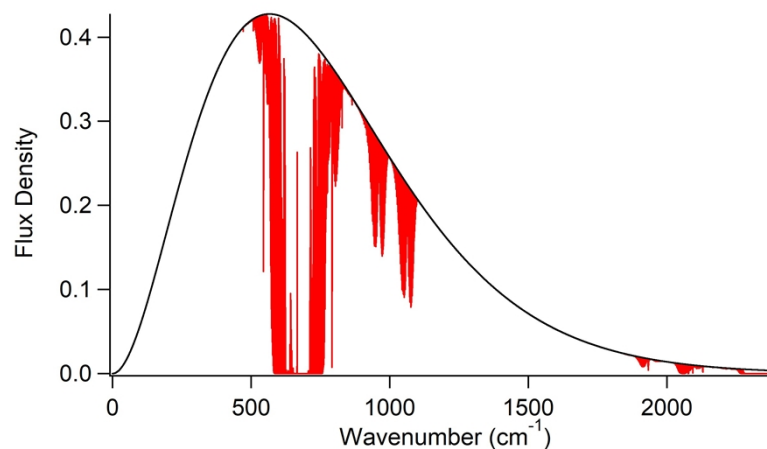
348 We can obtain the molar absorptivity of the CO_2 transitions from spectral measurements of
349 infrared absorption bands of CO_2 , which have been tabulated in the HITRAN database.[58] Similar
350 calculations are possible for other energy-absorbing gases such as H_2O and CH_4 . Methane is an
351 increasing concern because of the large amount of this gas trapped in permafrost that will be

352 released as warming continues creating a greater forcing. However, methane plays a relatively
353 minor role today, compared to CO_2 . We will include H_2O as a constant because it plays a major
354 role in feedback processes and is important to any approximate model of atmospheric
355 transmittance.

356 Results

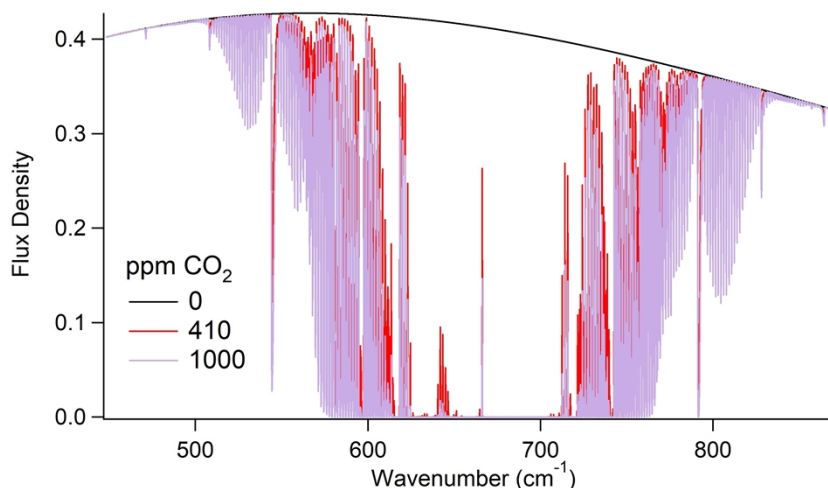
357 *Calculation of the effect of an energy absorbing gas on the transmittance of surface radiation*

358 In order to implement the CO_2 -only model as a predictive broadband steady-state model
359 for absorption by the atmosphere, we can use the transmittance in the range $250 - 1990\text{ cm}^{-1}$. The
360 Planck curve initially has the following appearance, i.e. when $P_{CO_2} = 420\text{ ppm}$.



361
362 Figure 3. Planck thermal emission of the earth (black) assuming a surface temperature of 288 K compared
363 to the emission combined with the transmission spectrum of CO_2 obtained from the HITRAN database
364 (red).

365 The region between $250 - 1990\text{ cm}^{-1}$ has been plotted as transmittance at 410 and 1000 ppm for
366 comparison in Figure 4.



367

368

Figure 4. Comparison of the transition spectrum of CO₂ at 410 and 1000 ppm.

369

The average transmittance in the entire region shown in Figure 3 was used to estimate the change in transmittance across the Planck curve. We assumed that there is no significant change below 250 cm⁻¹ or above 1990 cm⁻¹ for this CO₂-only model. The Planck curve and each modified Planck curve with CO₂ transmittance included were integrated numerically. Then the ratio of the integrated flux is taken to obtain the transmittance at a given value of CO₂ ppm (see Supporting Information).

374

375 *Consideration of the transmittance of water vapor*

376

In order to approximate the effect of H₂O vapor on the CO₂ absorption, we use the fact that transmittances are multiplicative.

377

378

$$\tau_{atm} = \tau_{H_2O} \tau_{CO_2} \quad (9)$$

379

For relatively small changes in the of ppm of CO₂ we can treat the H₂O transmittance as a constant and estimate that the decrease in total transmitted intensity as

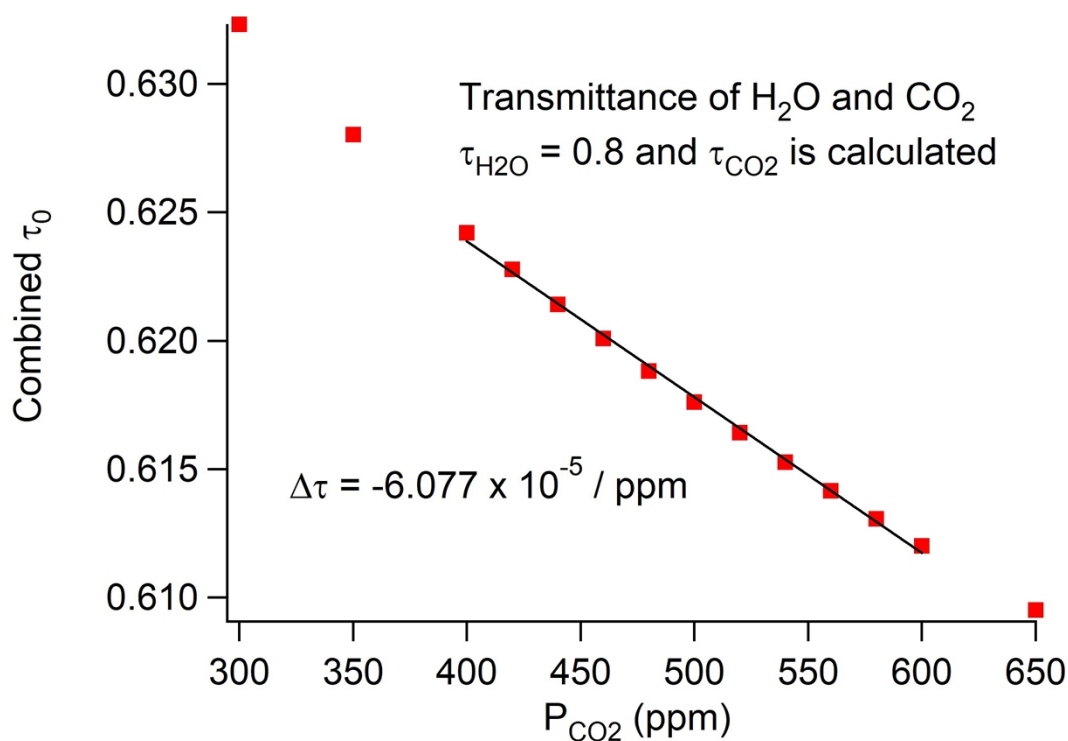
380

381

$$\frac{\delta \tau_{atm}}{\delta ppm} \cong \tau_{H_2O} \frac{\delta \tau_{CO_2}}{\delta ppm} \quad (10)$$

382 The H₂O transmittance is a constant multiplicative factor because H₂O is relatively constant in the
383 atmosphere (although it has cyclic variation in feedback loops), while CO₂ transmittance decreases
384 as can be seen graphically in Figures 3 and 4.

385 The relative change due to CO₂ obtained from the calculated transition of HITRAN data
386 was multiplied by an assumed $\tau_{H_2O} = 0.80$ in order to include the effect of H₂O and all other gases
387 that absorb the earth's thermal emission to create the line shown in Figure 5. According to this
388 model, CO₂ by itself accounts for ~20 % of the reduction in transmittance of the atmosphere at
389 present.



390
391 Figure 5. Global average transmittance of energy-absorbing gases. It was assumed that the transmittance
392 due to all gases other than CO₂ was 0.80 and the differential effect and slope of the line is due only to
393 CO₂. The model separates the effects of CO₂ from those other gases.

394 The change in the transmittance as a function of CO₂ ppm obtained from the regression line in
395 Figure 5 is given by

$$396 \quad \tau_{atm} = 0.648 - 6.077 \times 10^{-5} ppm \quad (11)$$

397 *The role of transmittance in the radiation equilibrium model*

398 The model treats the earth's surface with no distinction between land, ocean or atmosphere,
399 except that the atmosphere is an energy-absorbing layer that reduces the flux that escapes to space.
400 The basis of the model used to calculate the temperature of the earth is that the incident radiation
401 flux from the sun equals the flux from the earth. [59]

$$402 \quad F_{solar} = F_{bare\ earth} \quad (12a)$$

403 When the atmosphere is included it must still be true that the radiation leaving the earth at
404 the TOA is equal to the solar flux.

$$405 \quad F_{solar} = F_{TOA} \quad (12b)$$

406
407 In order to maintain radiation equilibrium between the sun and earth, the radiation emitted
408 from the TOA must be the same as the radiation emitted by the surface of the bare earth, i.e. the
409 earth without the atmosphere. This also follows from Eqns. 12a and b.

$$410 \quad F_{TOA} = F_{bare\ earth} \quad (12c)$$

411 Next, we assume that the flux at the top of the atmosphere is reduced by the transmittance of the
412 atmosphere that we calculated above.

$$413 \quad F_{TOA} = F_{atm} \quad (13)$$

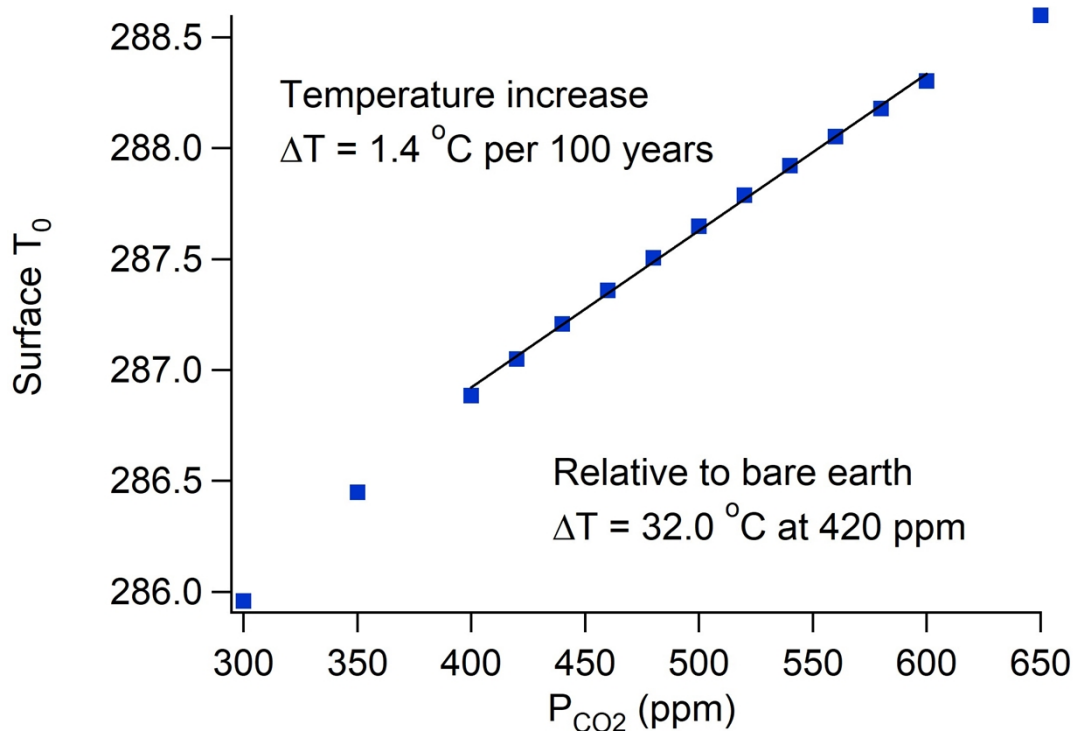
414 Since we can calculate $F_{bare\ earth}$ we can solve for the flux at the surface of the earth surrounded
415 by an absorbing atmosphere, F_{atm} . Since $\tau_{TOA} < 1$, the requirement for radiation balance at the top
416 of the atmosphere at equilibrium requires the flux at the earth's surface to be larger than the flux
417 of at top of the atmosphere. At equilibrium with a fixed amount of energy absorbing gas we have

$$418 \quad F_{atm} = \frac{F_{bare\ earth}}{\tau_{TOA}} \quad (14)$$

419 Therefore, when the Stefan-Boltzmann law is applied $\sigma T_{atm}^4 \tau_{TOA} = \sigma T_{bare\ earth}^4$, and

$$420 \quad T_{atm} = \frac{T_{bare\ earth}}{\sqrt[4]{\tau_{TOA}}} \quad (15)$$

421 Figure 6 shows the result of this calculation. Since $T_{bare\ earth} = 255$ K, the equilibrated surface
422 temperature of the earth surrounded by an atmosphere of CO₂ at 410 ppm is $T_{atm} = 285.4$ K.
423 According to NOAA the average temperature over the past 10 years has been 13.9 °C or 288.9 K.
424 Clearly, using only natural abundance CO₂ and neglecting all other greenhouse gases will give a
425 lower bound. However, the main point of this calculation is to estimate the rate of change of
426 transmittance and temperature as the CO₂ partial pressure increases.



427

428 Figure 6. The correlation between the partial pressure of CO_2 in the atmosphere and the surface temperature
429 calculated using radiation equilibrium while also accounting for the transmittance of the atmosphere.

430 The temperature increase compared to bare earth is $32.0\text{ }^\circ C$ because of the greenhouse effect. The
431 calculated warming since the earliest tabulated values in P_{CO_2} to the present is $1.1\text{ }^\circ C$. Current
432 estimates of the warming in the atmosphere and ocean since the beginning of the industrial
433 revolution are $1.0\text{ }^\circ C$ and $0.8\text{ }^\circ C$, respectively. The ocean is the long-term heat sink because of its
434 larger mass and much higher heat capacity. Thus, the calculated value compares well with either
435 atmospheric or oceanic temperature changes. The model predicts that the surface temperature will
436 have increased on average by an additional $1.4\text{ }^\circ C$ when 600 ppm is reached. This would occur in
437 the early 22nd century at the current rate of emission of CO_2 . The model predicts an annual increase
438 of $0.014\text{ }^\circ C$, which agrees with sophisticated climate models.

439 **Discussion**

440 There are many details that have been neglected in the radiation model described above. A
441 detailed treatment of the energy balance by radiative transfer in the atmosphere would include
442 reflection, transmission, and absorption of layers of atmosphere to account for changing pressures,
443 temperature, and composition with altitude. Computer simulations are based on the above factors
444 combined with the effects of radiative transfer, convection, and Coriolis forces as well as ocean
445 currents, gas exchange and convection, but also absorption by other gases such as CH₄, O₃ and
446 N₂O, H₂O feedback and scattering by aerosols. Although these are all important aspects, we only
447 need the Planck radiation law and data for CO₂ absorption to obtain the fundamental result from
448 the most important forcing term, P_{CO_2} . We have chosen the HITRAN database to calculate the
449 transmittance in Eqn. (8) because it is the most complete and accessible to the public. Since the
450 concentration of H₂O is variable in the atmosphere, we have assumed a cross-sectional number
451 density that gave a reasonable agreement with the temperature trend. These parameters were used
452 in an Excel spreadsheet provided in the Supporting Information. The HITRAN data for CO₂ were
453 processed by summing Gaussian peaks with a linewidth of 0.13 cm⁻¹. Circa 67,700 transitions were
454 used as input and the processed spectral data file consisted of 240,000 evenly spaced points from
455 0.01 to 2,400 cm⁻¹. Excel and IgorPro can easily manage these arrays. These materials are available
456 in the Supporting Information. The Excel spreadsheet contains the spectra data in column B
457 (Figure 2), the transmittance data in column I, the Planck distribution in column K and the product
458 of the transmittance with the Planck distribution in column L (Figure 3). The spreadsheet allows
459 calculation atmospheric transmittance and temperature for an input P_{CO_2} . In the final column (M)
460 the integrated flux distributions with and without CO₂ are compared, the total transmittance of the
461 atmosphere is calculated (with H₂O transmittance as a constant multiplier) and the temperature of
462 the earth for a given CO₂ ppm is calculated according to Eqn. (15). Changes to the CO₂ linewidth

463 and H₂O cross-sectional number density cannot alter the inescapable conclusion that increasing
464 P_{CO_2} results in an increase in the temperature of the earth's surface.

465 Scientists have previously attempted to calculate the forcing term due to CO₂ with similar
466 motivation, namely to illustrate the energy-absorbing effect of CO₂. In the 1960s, Stull, Wyatt and
467 Plass used the data available at that time to estimate the absorbance using a statistical approach to
468 determining the absorbance of segments of the CO₂ spectrum that had a width of 10 cm⁻¹ or 50 cm⁻¹.
469 [56] A statistical method was used because only the most intense CO₂ bands had been tabulated
470 and the researchers were aware that there were numerous isotopologues and the Fermi resonance
471 effect that created a congested spectrum.[56] Today, There is no longer a need for the
472 complications of a statistical model since the CO₂ absorption lines are available from the HITRAN
473 database. The HITRAN database also permits calculations that include isotopes of CO₂ and
474 consideration of other greenhouse gases such as CH₄ and O₃. These are easy to implement by the
475 methods used here, merely by selecting the spectral intensities corresponding to those species in
476 the output from the HITRAN database, which has more than one million entries for CO₂ and its
477 isotopologues.

478 There are three mechanisms by which the excited CO₂ can lose its absorbed energy:
479 collisional deactivation, spontaneous emission, and stimulated emission. We can ignore
480 spontaneous emission. In the text, "Atmospheric Radiation"[60] by Goody and Yung, the
481 collisional lifetime of excited carbon dioxide is estimated to be 25 microseconds when the pressure
482 is 1 bar and the temperature is 180 K. Even where the pressure of the atmosphere is 0.008 bar,
483 near its lowest point, at 32 km and at 217 K, the collisional lifetime is 2 milliseconds while the
484 spontaneous decay half-life of carbon dioxide in the first bending mode excited state is estimated
485 to be about 0.75 seconds.[60] Thus, even at 32 km, where the ratio has its minimum value, there

486 are about 375 collisional deactivations for every spontaneous emission. Stimulated emission
487 makes a small contribution given that the equilibrium constant for population of the vibrational
488 excited state of the CO₂ bending mode is relatively small and only ~ 3.7 % is populated at 298 K.
489 Collisional deactivation dominates leading to dissipation of absorbed radiation as heat.
490 Collectively, the molecules of the atmosphere also radiate as a thermal body, which should be
491 considered in a detailed radiation equilibrium model.[61,62] We include the thermal radiation by
492 the atmosphere itself as part of the total radiation from the earth's surface. This is clearly an
493 enormous simplification.

494 The transmittance model based on the best available spectroscopic data show that CO₂
495 absorption in the atmosphere is saturated in the central region of the spectrum, but not in the
496 flanking regions. Indeed, we can estimate that CO₂ will approach total saturation only when the
497 partial pressure reaches many thousands of ppm, although it begins to depart from linearity at less
498 than 600 ppm. There are many CO₂ bands, including the rovibrational progression and Fermi
499 resonance bands, which are thermally populated to different extent. While the center of the
500 transition, the Q-branch and most intense portions of the P and R branches are saturated, there are
501 thousands of absorption bands that have sufficient concentration-dependent absorption intensity
502 to act as a significant radiative forcing that increases the internal energy of atmosphere. Increasing
503 P_{CO_2} results in decreasing transmittance which in turn increases the temperature at the surface of
504 the earth. Despite its simplicity the radiation equilibrium model is quite accurate regarding the
505 change in temperature, which is of greatest interest. The Keeling curve shows that P_{CO_2} increases
506 at a rate of 2.1 ppm/year. At this rate, global P_{CO_2} will increase from its current value of 410 ppm
507 to 600 ppm in 90 years. According to the radiation calculations using either method developed
508 here, the temperature is predicted to increase by approximately 1.4 °C over this time. This is an

509 entirely reasonable estimate when compared to more sophisticated models. The methods given
510 here can be implemented by non-specialists to help them understand the imbalances in the system
511 caused by a forcing, which is one of the foundations for climate system modeling.

512 The method implemented here provides a simple way to compare the energy-absorbing gas
513 effect and its consequences with studies by critics of climate sciences.[63] The work by Schmidt
514 and co-workers suggests that H₂O absorption swamps out CO₂ and that doubling the current P_{CO_2}
515 would have little effect on the temperature. Using data from the HITRAN database processed by
516 either an Excel spreadsheet or python code those claims could be put to the test. Based on evidence
517 we can establish a correlation between P_{CO_2} increase and temperature rise. The data are the Keeling
518 curve, the mass of the atmosphere, the earth's radius, the solar radius, and the temperature of the
519 sun.

520 The issue we have addressed in this paper is the fact that chemists, physicists, and other
521 non-climatologists are at a disadvantage in invoking climate-science computer models as evidence
522 of changes in the energy balance of the earth and its atmosphere. The intent of the analytical
523 approach to the energy-absorbing gas phenomenon is not to replace these detailed studies, but
524 rather to make non-specialists aware of fundamental reasoning associated with interpretation of
525 climate science that are often poorly understood by the public. The Excel spreadsheet is entirely
526 based spectroscopy, geometry, and radiation physics that is taught at the undergraduate level in
527 several disciplines. It is rarely taught in a cohesive manner that covers all aspects in each discipline
528 because of crowded curricula. The model and calculation are a proposed remedy for those who
529 feel that the subject of climate change deserves more attention in teaching and research.

530 **Conclusion**

531 We believe that the approach shown here and in the spreadsheet tool will be of value
532 because many scientists have a reluctance to base a statement on a “black box” argument. It is not
533 because of mistrust in the results, but rather that non-specialists do not feel sufficiently well versed
534 in the methods to explain or defend the predictions of modeling or simulations that they have not
535 conducted themselves. The model presented here provides chemists, physicists, and other
536 interested scientists a demonstration of the effect of atmospheric absorbance on the surface
537 temperature based on the fundamentals of spectroscopy and the theory of thermal radiation in its
538 most elementary form, the Stefan-Boltzmann law. While the general concept of a *greenhouse gas*
539 is widely understood, the correlation of CO₂ as an energy-absorbing gas with an increase in
540 terrestrial temperature is best described using a quantitative model. It is gratifying that this model
541 has stood the test of time since Arrhenius published a version of it in 1896, albeit with much more
542 limited data.

543

544 **Availability of Data and Materials Declaration**

545 All materials will be made available on request. At present they are posted on a website located
546 at: <http://stemed.site/NCSU/Research/atm/index.html>.

547 **Funding Declaration**

548 The authors did not receive support from any organization for the submitted work.

549 **Ethics Approval**

550 We understand and abide by the ethical guidelines of the journal.

551 **Consent to Participate**

552 Both authors consented to collaborate on this work in advance of the writing of the manuscript.

553 **Consent for Publication**

554 Both authors are aware of and support publication of this manuscript.

555 **Competing Interest Declaration**

556 The authors declare no competing interests.

557 **Author Contributions**

558 The authors contributed equally to this manuscript. Both were involved in the writing. Hugo.
559 Franzen provided the radiation equilibrium methods, geometrical, and physical chemistry,
560 aspects. Stefan Franzen provided spectroscopic applications, developed tools to use
561 spectroscopic data, wrote all codes and made the figures.

562 **Supporting Information**

563 The supporting information consists of a differential flux method for determining the surface
564 temperature of the Earth and the increase proportional to the CO₂ ppm increase in both an Excel
565 and IgorPro spreadsheet. A parallel approach to the same data processing is provided in Python
566 scripts. These are all given on the website: <http://stemed.site/NCSU/Research/atm/index.html>.
567 The topics are numbered.

- 568 1. Theoretical intensities of CO₂ transitions
- 569 3. Methods for spectral calculations, flux, and effect of linewidth
- 570 3. Fortran programs for calculating the geometrically averaged line shapes
- 571 4. Atmospheric temperature increase as result of CO₂ increase (differential flux method)
- 572 5. Earth_Temperature Spreadsheet, Earth_Temperature_Spreadsheet.pdf and Python scripts
573 that demonstrate the columns of the spreadsheet graphically and follow each step of the
574 derivation from HITRAN CO₂ absorption bands to CO₂ transmittance and finally surface
575 temperature of the Earth.

576

577

578 **References**

- 579 1. de Oliviera Andrade R (2019) Alarming surge in Amazon fires prompts global outcry. Nature News
580 Aug. 23.
- 581 2. Pierre-Louis K, Schwartz J (2020) Why Does California Have So Many Wildfires? New York Times
582 Dec. 3.
- 583 3. Cornwall W (2019) Ocean heat waves like the Pacific’s deadly ‘Blob’ could become the new normal.
584 Science Magazine Jan. 31.
- 585 4. Fox D (2020) Biggest ice sheet on Earth more vulnerable to melting than thought. National Geographic
586 Jul. 22.
- 587 5. Walker XJ, Baltzer JL, Cumming SG, Day NJ, Ebert C, et al. (2019) Increasing wildfires threaten
588 historic carbon sink of boreal forest soils. Nature 572: 520-523.
- 589 6. Amigo I (2020) When will the Amazon hit a tipping point? Nature News Feb. 25.
- 590 7. Fischer D (2011) Federal Investigators Clear Climate Scientist, Again. Scientific American Aug. 23.
- 591 8. Planck M (1901) Law of energy distribution in normal spectra. Annalen Der Physik 4: 553-563.
- 592 9. Boltzmann L (1884) Ableitung des Stefan'schen Gesetzes, betreffend die Abhängigkeit der
593 Wärmestrahlung von der Temperatur aus der electromagnetischen Lichttheorie. [Derivation of
594 Stefan's law, concerning the dependency of heat radiation on temperature, from the
595 electromagnetic theory of light]. Annalen der Physik und Chemie 258: 291–294.
- 596 10. Das B (2002) Obtaining Wien's displacement law from Planck's law of radiation The Physics Teacher
597 40: 148-149.
- 598 11. Mudge FB (1997) The development of the ‘greenhouse’ theory of global climate change from
599 Victorian times Weather 52: 13-17.
- 600 12. Arrhenius S (1896) On the Influence of Carbonic Acid in the Air upon the Temperature of Ground.
601 Phil Mag and J of Sci 41: 237-276.

- 602 13. Ramanathan V, Vogelmann AM (1997) Greenhouse effect, atmospheric solar absorption and the
603 Earth's radiation budget: From the Arrhenius-Langley era to the 1990s. *Ambio* 26: 38-46.
- 604 14. Very FW (1913) The Temperature Assigned by Langley to the Moon. *Science* 37: 949-957.
- 605 15. Angstrom K (1900) Ueber die Bedeutung des Wasserdampfes und der Kohlemaure bei der
606 Absorptiom der Erdatmosphare. *Annalen Der Physik* IV: 720-732.
- 607 16. Callendar GS (1938) The artificial production of carbon dioxide and its influence on temperature.
608 *Quarterly Journal of the Royal Meteorological Society* 64: 223-240.
- 609 17. Martin PE, Barker EF (1932) The infrared absorption spectrum of carbon dioxide. *Physical Review*
610 41: 291-303.
- 611 18. Kaplan LD (1947) The Absorption Spectrum of Carbon Dioxide From 14 to 16 Microns. *J Chem Phys*
612 15: 809-815.
- 613 19. Keeling C (1960) The concentration and isotopic abundances of carbon dioxide in the atmosphere.
614 *Tellus Series B-Chemical and Physical Meteorology* 12: 200–203.
- 615 20. Shindell DT, Schmidt GA, Miller RL, Mann ME (2003) Volcanic and solar forcing of climate change
616 during the preindustrial era. *Journal of Climate* 16: 4094-4107.
- 617 21. Paterson NR (2011) Global Warming: A Critique of the Anthropogenic Model and its Consequences.
618 *Geoscience Canada* 38: 41-48.
- 619 22. Christy JR, Herman B, Pielke R, Klotzbach P, McNider RT, et al. (2010) What Do Observational
620 Datasets Say about Modeled Tropospheric Temperature Trends since 1979? *Remote Sensing* 2:
621 2148-2169.
- 622 23. Lloyd EA (2012) The role of 'complex' empiricism in the debates about satellite data and climate
623 models. *Studies in History and Philosophy of Science* 43: 390-401.
- 624 24. IPCC (2013) Box TS.3: Climate Models and the Hiatus in Global Mean Surface Warming of the Past
625 15 Years. *Climate Change: Technical Summary*: 61-63.
- 626 25. Kosaka Y, Xie SP (2013) Recent global-warming hiatus tied to equatorial Pacific surface cooling.
627 *Nature* 501: 403-407.

- 628 26. Meehl GA, Arblaster JM, Fasullo JT, Hu AX, Trenberth KE (2011) Model-based evidence of deep-
629 ocean heat uptake during surface-temperature hiatus periods. *Nature Climate Change* 1: 360-364.
- 630 27. Mauritsen T, Bader J, Becker T, Behrens J, Bittner M, et al. (2019) Developments in the MPI-M Earth
631 System Model version 1.2 (MPI-ESM1.2) and Its Response to Increasing CO₂. *Journal of*
632 *Advances in Modeling Earth Systems* 11: 998-1038.
- 633 28. McNeall D, Williams J, Betts R, Booth B, Challenor P, et al. (2020) Correcting a bias in a climate
634 model with an augmented emulator. *Geoscientific Model Development* 13: 2487-2509.
- 635 29. Tang Q, Klein SA, Xie SC, Lin WY, Golaz JC, et al. (2019) Regionally refined test bed in E3SM
636 atmosphere model version 1 (EAMv1) and applications for high-resolution modeling.
637 *Geoscientific Model Development* 12: 2679-2706.
- 638 30. Drake JB, Jones PW, Carr GR (2005) Overview of the software design of the Community Climate
639 System Model. *International Journal of High Performance Computing Applications* 19: 177-186.
- 640 31. Flynn CM, Mauritsen T (2020) On the climate sensitivity and historical warming evolution in recent
641 coupled model ensembles. *Atmospheric Chemistry and Physics* 20: 7829-7842.
- 642 32. Gier BK, Buchwitz M, Reuter M, Cox PM, Friedlingstein P, et al. (2020) Spatially resolved
643 evaluation of Earth system models with satellite column-averaged CO₂. *Biogeosciences* 17:
644 6115-6144.
- 645 33. Mann ME, Miller SK, Rahmstorf S, Steinman BA, Tingley M (2017) Record temperature streak bears
646 anthropogenic fingerprint. *Geophysical Research Letters* 44: 7936-7944.
- 647 34. Raisanen J, Ylhaisi JS (2015) CO₂-induced climate change in northern Europe: CMIP2 versus CMIP3
648 versus CMIP5. *Climate Dynamics* 45: 1877-1897.
- 649 35. UCAR (2016) Overview of Community Climate System Model (CCSM). University Corporation for
650 Atmospheric Research <http://www.cesm.ucar.edu/about/>.
- 651 36. McGuffie K, Henderson-Sellers A (2001) Forty years of numerical climate modelling. *International*
652 *Journal of Climatology* 21: 1067-1109.

- 653 37. Goosse H, Arzel O, Luterbacher J, Mann ME, Renssen H, et al. (2006) The origin of the European
654 "Medieval Warm Period". *Climate of the Past* 2: 99-113.
- 655 38. Delworth TL, Broccoli AJ, Rosati A, Stouffer RJ, Balaji V, et al. (2006) GFDL's CM2 global coupled
656 climate models. Part I: Formulation and simulation characteristics. *Journal of Climate* 19: 643-
657 674.
- 658 39. Jonko AK, Shell KM, Sanderson BM, Danabasoglu G (2012) Climate Feedbacks in CCSM3 under
659 Changing CO2 Forcing. Part I: Adapting the Linear Radiative Kernel Technique to Feedback
660 Calculations for a Broad Range of Forcings. *Journal of Climate* 25: 5260-5272.
- 661 40. Phipps SJ, Rotstayn LD, Gordon HB, Roberts JL, Hirst AC, et al. (2012) The CSIRO Mk3L climate
662 system model version 1.0-Part 2: Response to external forcings. *Geoscientific Model
663 Development* 5: 649-682.
- 664 41. Tachiiri K, Hargreaves JC, Annan JD, Oka A, Abe-Ouchi A, et al. (2010) Development of a system
665 emulating the global carbon cycle in Earth system models. *Geoscientific Model Development* 3:
666 365-376.
- 667 42. Andrews T, Forster PM, Gregory JM (2009) A Surface Energy Perspective on Climate Change.
668 *Journal of Climate* 22: 2557-2570.
- 669 43. Hansen J, Nazarenko L, Ruedy R, Sato M, Willis J, et al. (2005) Earth's energy imbalance:
670 Confirmation and implications. *Science* 308: 1431-1435.
- 671 44. Etminan M, Myhre G, Highwood EJ, Shine KP (2016) Radiative forcing of carbon dioxide, methane,
672 and nitrous oxide: A significant revision of the methane radiative forcing. *Geophysical Research
673 Letters* 43: 12614-12623.
- 674 45. Goosse H, Cresspin E, Dubinkina S, Loutre MF, Mann ME, et al. (2012) The role of forcing and
675 internal dynamics in explaining the "Medieval Climate Anomaly". *Climate Dynamics* 39: 2847-
676 2866.
- 677 46. Kiehl JT, Trenberth KE (1997) Earth's annual global mean energy budget. *Bulletin of the American
678 Meteorological Society* 78: 197-208.

- 679 47. Mann ME (2007) Climate over the past two millennia. *Annual Review of Earth and Planetary*
680 *Sciences* 35: 111-136.
- 681 48. Mann ME, Schmidt GA (2003) Ground vs. surface air temperature trends: Implications for borehole
682 surface temperature reconstructions. *Geophysical Research Letters* 30. No. 12, 1607
- 683 49. Myhre G, Highwood EJ, Shine KP, Stordal F (1998) New estimates of radiative forcing due to well
684 mixed greenhouse gases. *Geophysical Research Letters* 25: 2715-2718.
- 685 50. Anderson GP, Kneizys FX, Chetwynd JH, Rothman LS, Hoke ML, et al. (1996) Reviewing
686 atmospheric radiative transfer modeling: New developments in high and moderate resolution
687 FASCODE/FASE and MODTRAN; Hays PB, Wang JX, editors. 82-93 p.
- 688 51. Keeling CD, Piper SC, Bacastow RB, Wahlen M, Whorf TP, et al. (2005) Atmospheric CO₂ and
689 ¹³CO₂ exchange with the terrestrial biosphere and oceans from 1978 to 2000: observations and
690 carbon cycle implications. *A History of Atmospheric CO₂ and its effects on Plants, Animals, and*
691 *Ecosystems* editors, Ehleringer, J.R., T. E. Cerling, M. D. Dearing, Springer Verlag, New York:
692 83-113.
- 693 52. Wunch D, Toon GC, Blavier JFL, Washenfelder RA, Notholt J, et al. (2011) The Total Carbon
694 Column Observing Network. *Philosophical Transactions of the Royal Society a-Mathematical*
695 *Physical and Engineering Sciences* 369: 2087-2112.
- 696 53. Zhong WY, Haigh JD (2013) The greenhouse effect and carbon dioxide. *Weather* 68: 100-105.
- 697 54. Herzberg G (1945) *Molecular Spectra and Molecular Structure II. Infrared and Raman Spectra of*
698 *Polyatomic Molecules*. van Nostrand Company, Princeton, New Jersey.
- 699 55. Fermi E (1931) The Raman effect of carbon dioxide. *Zeitschrift Fur Physik* 71: 250-259.
- 700 56. Wyatt PJ, Stull VR, Plass GN (1964) Infrared Transmittance of Carbon Dioxide. *Applied Optics* 3:
701 243-254.
- 702 57. Schildknecht D (2020) Saturation of the infrared absorption by carbon dioxide in the atmosphere.
703 *International Journal of Modern Physics B* 34.

- 704 58. Gordon IE, Rothman LS, Hill C, Kochanov RV, Tan Y, et al. (2017) The HITRAN2016 molecular
705 spectroscopic database. *Journal of Quantitative Spectroscopy & Radiative Transfer* 203: 3-69.
- 706 59. Trenberth KE, Fasullo JT, Kiehl J (2009) Earth's global energy budget. *Bulletin of the American*
707 *Meteorological Society* 90: 311-323.
- 708 60. Goody RM, Y LY (1989) *Atmospheric Radiation*. Oxford University Press, Oxford, UK.
- 709 61. Zhou YP, Kratz DP, Wilber AC, Gupta SK, Cess RD (2007) An improved algorithm for retrieving
710 surface downwelling longwave radiation from satellite measurements. *Journal of Geophysical*
711 *Research-Atmospheres* 112, D15102.
- 712 62. Gui S, Liang SL, Li L (2010) Evaluation of satellite-estimated surface longwave radiation using
713 ground-based observations. *Journal of Geophysical Research-Atmospheres* 115, D18214.
- 714 63. Schmidt GA, Ruedy RA, Miller RL, Lacis AA (2010) Attribution of the present-day total greenhouse
715 effect. *Journal of Geophysical Research-Atmospheres* 115, D20106.